

ANALYSIS OF LAYERS DEPOSITED ON 10CrMo9-10 STEEL AFTER CO-COMBUSTION OF COAL AND BIOMASS

Michał OPYDO¹, Agata DUDEK¹, Grzegorz GOLANŃSKI¹, Paweł URBAŃCZYK²

¹ Czestochowa University of Technology, Faculty of Production Engineering and Materials Technology, Institute for Material Engineering,

Al. Armii Krajowej 19, 42-200 Czestochowa, e-mail: opydomichal@wip.pcz.pl

² Office of Technical Inspection, Division in Dabrowa Gornicza, Poland

Summary

Energy market is the sector of the economy which has been given a lot of attention in the last decades. This results not only from a global increase in demand for energy but also from the needs for environmental protection. It should be also noted that modernization of the energy sector is capital-intensive. Therefore, the directions of development in this sector should be driven not only by ecological reasons but also by reasonable economic calculus based on in-depth analysis of operational costs in the next decades. For this reason, an important position in the structure of energy generation is taken by co-combustion of various fuels, with particular focus on coal and biomass. Co-combustion of fuel mixtures, with each fuel having varied properties, often accelerates degradation of the structural components of a boiler.

Keywords: energy sector, biomass, co-combustion, surface degradation, steam superheater.

ANALIZA OSADÓW POWSTAŁYCH NA STALI 10CrMo9-10 W WYNIKU WSPÓLSPALANIA WĘGLA I BIOMASY

Streszczenie

Energetyka w ostatnich dziesięcioleciach jest jedną z tych gałęzi gospodarki, której poświęca się bardzo dużo uwagi. Wynika to nie tylko z globalnego wzrostu zapotrzebowania na energię, ale także z potrzeby ochrony środowiska naturalnego. Jednocześnie należy pamiętać, że modernizacja energetyki jest bardzo kapitałochłonna, dlatego też o kierunkach rozwoju branży muszą decydować nie tylko względy ekologiczne, ale także przemyślany rachunek ekonomiczny oparty na dogłębnej analizie kosztów eksploatacyjnych elektrowni w następnych dekadach. Z tego powodu znaczącą pozycję w strukturze produkcji energii zajmuje współspalanie różnych paliw, głównie węgla i biomasy. Spalanie mieszaniny paliw, z których każde odznacza się zróżnicowanymi właściwościami, często skutkuje przyspieszoną degradacją elementów konstrukcyjnych kotła.

Słowa kluczowe: energetyka, biomasa, współspalanie, degradacja powierzchni, przegrzewacz pary.

1. INTRODUCTION

Sustainable development needs a strong industry supported with the efficiently operating energy sector. For this reason, the attempts are constantly made to maximize the efficiency in this segment of the economy. Development in the energy sector, however, involves numerous threats, such as dynamically growing demand for electricity in developing countries, decreasing resources of fossil fuels (coal, crude oil, natural gas) and policies of the European Union concerning minimization of carbon dioxide emissions [1-5]. Therefore, the tendencies aimed at increasing the efficiency of new installations and optimization of fuel consumption used in power plants have been observed.

Materials used for construction of energy installations are being incessantly modified to meet

the demands of having properties suitable for working under specific operating conditions, such as elevated temperature, steam pressure and type of fuel and to ensure long life of the equipment. Improperly chosen fuel might accelerate corrosion and degradation of steel components of boilers [6, 7].

This study presents the results of the studies aimed at analysis of the process of degradation of the surface of steam superheater made of 10CrMo9-10 (10H2M). This component operated for a long time in a power plant unit, with its combustion chamber fuelled by the mixture of coal and biomass in the form of sunflower husk pellet.

2. THE MATERIALS AND OPERATING CONDITIONS

The material used for the examinations presented in this study was a part of the tube elbow cut out as a specimen during the periodical maintenance of the steam boiler of a combined heat and power plant with high power output (OP-140). The basic information concerning the boiler is contained in the Table 1. Total time of operation of the part of the tube in the boiler was estimated at 230,000 hours.

During this time, the boiler was heated with coal, whereas in the last 33,000 hours, with coal with insignificant (around 10%) content of biomass (sunflower husk pellet). Parameters of fuels used during operation are illustrated in Table 2.

Installation was comprised of smooth tubes, made of 10CrMo9-10 alloy steel used for construction of pressure components for operation at high temperatures. Chemical composition of the steel was presented in Table 3.

Table 1. The basic technical specification of OP-140 boiler

Parameter	Unit	Value
Net/gross power output	MW _t	112.6 / 125
Designed gross boiler efficiency	%	90.5
Outlet steam pressure	MPa	13.8
Outlet steam temperature	°C	540
Feed water pressure	MPa	16.2
Feed water temperature	°C	150

Table 2. Basic fuel parameters

Parameter	Unit	Value
<i>Coal</i>		
Calorific value	MJ/kg	22-23
Humidity	%	7-10
Ash	%	20-22
<i>Biomass (sunflower husk pellet)</i>		
Calorific value	MJ/kg	16-17
Humidity	%	10-16
Ash	%	2-4

Table 3. Chemical composition of specimens of the steel studied (% mass)

C	Mn	Si	P	S	Cu	Cr	Ni	Mo	Al
0,14	0,50	0,26	0,012	0,017	0,19	2,47	0,09	1,04	0,023

3. EXAMINATIONS AND METHODOLOGY

The aim of the analysis of degradation of 10CrMo9-10 steel was to carry out macro- and microscopic examinations. Observations of the microstructures and microareas were carried out on metallographical sections prepared in a conventional manner. Photographical documentation of the microstructures was made by means of Axiovert 25 optical microscope and JEOL JSM-6610LV scanning electron microscope.

EDX microanalyser integrated with the scanning electron microscope was used in order to analyse chemical composition of depositions. The chemical composition of the test steel was determined using a spectrometer Spectro Analytical Instrument K2.

X-ray quality analysis of the deposition was carried out using Seifert 3003 T-T diffractometer with a cobalt lamp with wavelength of 0.17902 nm. Heater current for the study was set at 40 mA, whereas voltage was 30 kV. The analysis was

carried out for the diffraction angles from 20 to 80°, with the angular step of 0.2°.

Hardness tests (Vickers method) were carried out in order to ensure greater precision for the analysis of deposition properties. Future-Tech FM-7 microhardness tester was used for these tests. The load used during the examinations was 980.7 mN.

4. RESULTS

The specimens analysed in the study represent a part of the boiler's steam coil in the superheater after long operation in a pulverized bed boiler in a combined heat and power plant. Combustion of coal in the boiler (and later, of mixture of coal and biomass) was a direct reason for growth of a deposited layer on the external surface of the superheater.

The examinations were carried out for the external surface (both in the front part and in the aerodynamic shadow) and in the cross-section of the specimen (see Fig. 1).

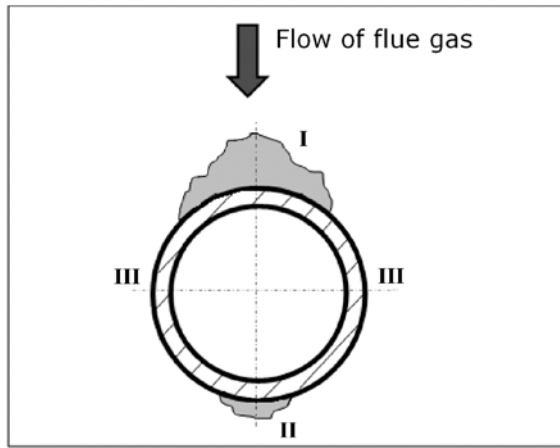


Fig. 1. Distribution of deposited layer on 10CrMo9-10 and diagram of the areas analysed

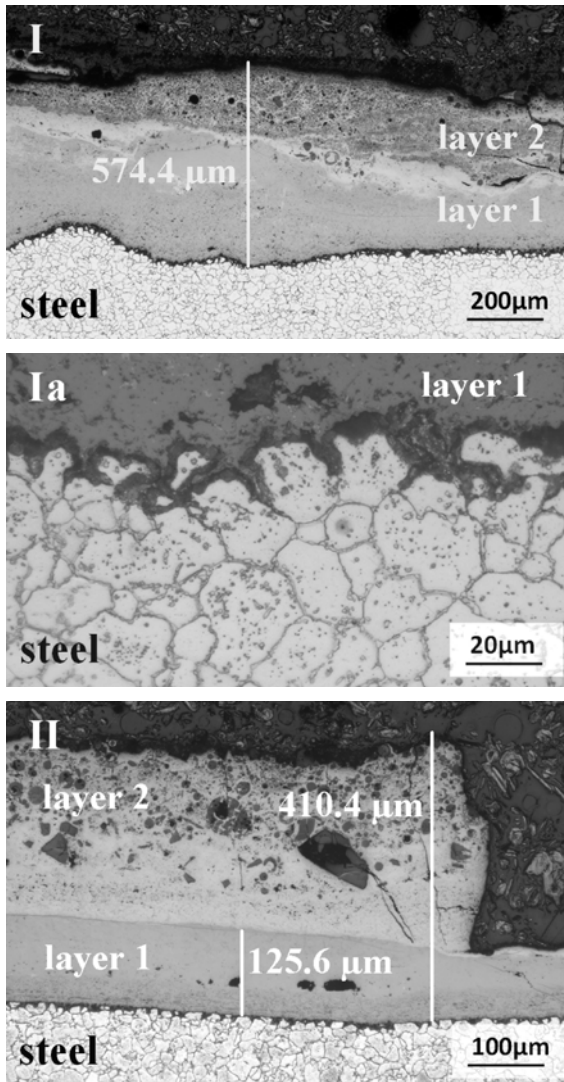


Fig. 2. Cross-section of the deposited layer on the external surface of steam superheater made of 10CrMo9-10 steel in the area I and area II

Selection of these areas was caused by presence of agglomerated depositions. The observations revealed that the thickest layer of deposition occurred in the frontal part (perpendicular to the direction of flue gas flow, area I). Maximal thickness of the deposited layer in this area was 1,432 μm .

On the opposite side of the specimen, (the aerodynamic shadow, area II), a deposited layer was found, reaching local thickness of 410.4 μm . In the zones where the direction of flue gas flow was parallel to the surface of the specimen (area III), thickness of the deposited layer was the lowest and ranged from 85 to ca. 100 μm (75 and 115 μm in extreme locations). The examples of cross-sections of the deposited layers are presented in the Figure 2.

The deposited layer formed in the front part was characterized by the most substantially developed surface. The most noticeable irregularity was also observed for the steel/deposition boundary line, which also represents the front of degradation of tube surface. In the area I, deposition was comprised of two layers with different morphology and properties. The first layer was characterized by a compact structure in the upper part and increased porosity in the boundary zone. The second layer showed substantially lower homogeneity of its structure.

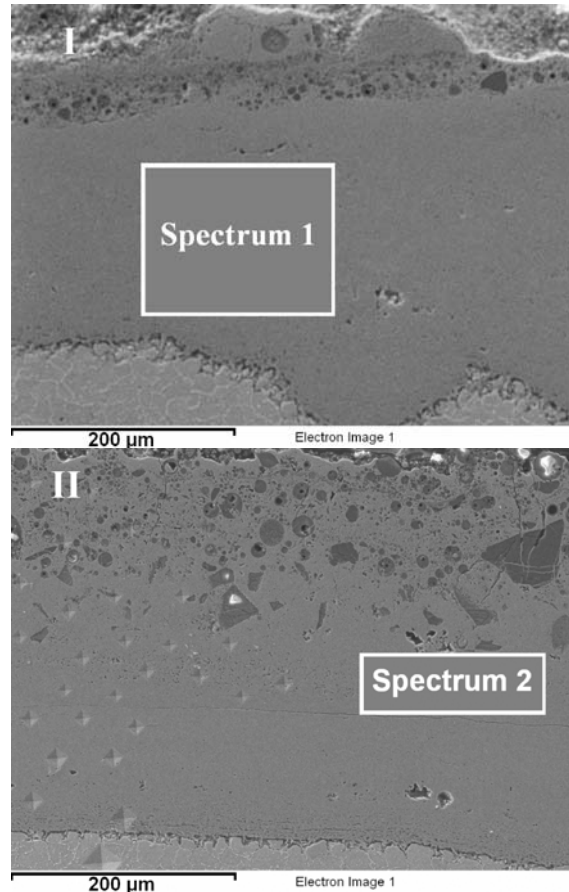


Fig. 3. Cross-section of the sample made of 10CrMo9-10 steel: in frontal part (I); in aerodynamic shadow (II)

With regard to the area in the aerodynamic shadow, the deposition also had two layers: their division and orientation with respect to steel surface showed high regularity. The first layer had a compact structure similar to the structure present in the major part of the specimen's perimeter (including the area III). Some inclusions were present in the second layer: large individual grains (with size over 15 μm) and fine dispersion grains (below 5 μm). In the second area, lower part of both layers was characterized by increased porosity.

Corrosion was observed in the area of steel/deposition boundary on grain boundaries (Ia). The penetration depth was evaluated at 20-25 μm

(maximum 40 μm) towards the depth from steel/deposition boundary.

The deposition formed on the steel and their structures were analysed by means of electron microscope. Analysis of the microstructure of the specimen studied supported the conclusions drawn from observations carried out by means of electron microscope. Example images recorded during the examination are presented in Fig. 3.

Chemical composition analysis was carried out during observations by means of scanning electron microscope. Analysis was conducted using EDX microanalyser coupled with scanning microscope. The results are presented in Table 4.

Table 4. Chemical composition of the depositions formed on the surface of 10CrMo9-10 steel after long operation, wt%

Area	K	S	Ca	Al	Si	Mg	Ti	Mn	Cr	Fe	Mo	Zn	C	O
<i>Frontal part</i>														
Layer 1	n/a	n/a	n/a	n/a	0.61	n/a	n/a	0.43	3.09	67.07	1.85	n/a	n/a	26.95
Layer 2	0.52	n/a	n/a	5.99	11.25	n/a	n/a	n/a	n/a	47.28	n/a	n/a	n/a	34.96
inclusion*	0.68	0.93	n/a	9.35	14.67	0.99	0.36	n/a	n/a	27.88	n/a	6.29	n/a	38.85
<i>Aerodynamic shadow</i>														
Layer 1	n/a	n/a	n/a	n/a	0.40	n/a	n/a	0.58	3.11	68.03	1.62	n/a	n/a	26.26
Layer 2	n/a	n/a	n/a	n/a	0.99	n/a	n/a	n/a	3.36	66.52	0.75	n/a	n/a	28.38
inclusion**	n/a	1.94	11.70	5.15	17.05	3.39	n/a	n/a	n/a	12.56	n/a	n/a	6.92	41.28

* chemical composition of the selected grain of inclusion present in the layer 2 of the area I, point analysis

** chemical composition of the selected grain of inclusion present in the layer 2 of the area II, point analysis

Co-combustion of coal and biomass in the boiler involved formation of the deposition with different chemical composition compared to the situation where only coal was combusted. Biomass is characterized by the substantially higher content of alkaline compounds [4, 8-11] (such as calcium, potassium or phosphorus), which directly affect chemical composition of the depositions formed. Presence of aggressive elements often leads to the increase in the rate of degradation of metal components of the boiler.

Analysis of the chemical composition (see Table 4) demonstrated that the external layers of the external layers of the deposited layer in both frontal part and in the aerodynamic shadow contain such elements as potassium, calcium, aluminium and magnesium. Absence of these elements in the chemical composition of the first layer was connected with operational history of the part of steam superheater analysed in the study: combustion of coal and biomass only in the last period of operation caused different characteristics of individual layers of the deposition. From the standpoint of the time of failure-free operation of the boiler, presence of sulphur is unfavourable. However, it should be noted that this element was not found in the layer formed directly on the steel core material.

Silicon was detected in each area of the deposited layer. Particularly high content of this element was found in the second layer, where silicon was responsible for numerous (usually high-dispersion) inclusions of the silicon oxides.

In the first layer, iron oxides were primarily present in both areas. Furthermore, the analysis revealed presence of manganese, chromium and molybdenum, which should be identified as alloy elements.

The next stage was X-ray quality analysis carried out by means of the diffractometer. Further analysis revealed mainly iron compounds present in the deposited layers (Fe_2O_3 , Fe_3O_4 and FeS), silicon dioxide (SiO_2) and complex compounds (CaAl_2O_4 , KNaCO_3). The results of phase analysis are presented in the form of diffractometers in Figure 4.

Specimen's hardness was also tested during the analysis; measurements with microhardness were carried out for both steel and individual deposited layers. The study demonstrated that steel hardness was at a medium level, ranging from 125.7 to 128.5 HV0.1. In the boundary zone (up to ca. 200 μm from steel/deposition boundary) steel showed elevated mean hardness: 133.8 HV0.1 for the first area and 139.6 HV0.1 for the second.

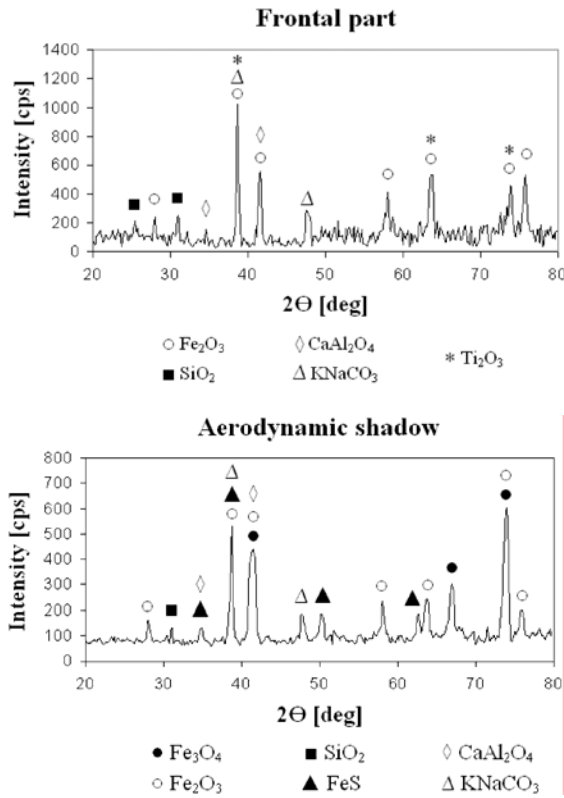


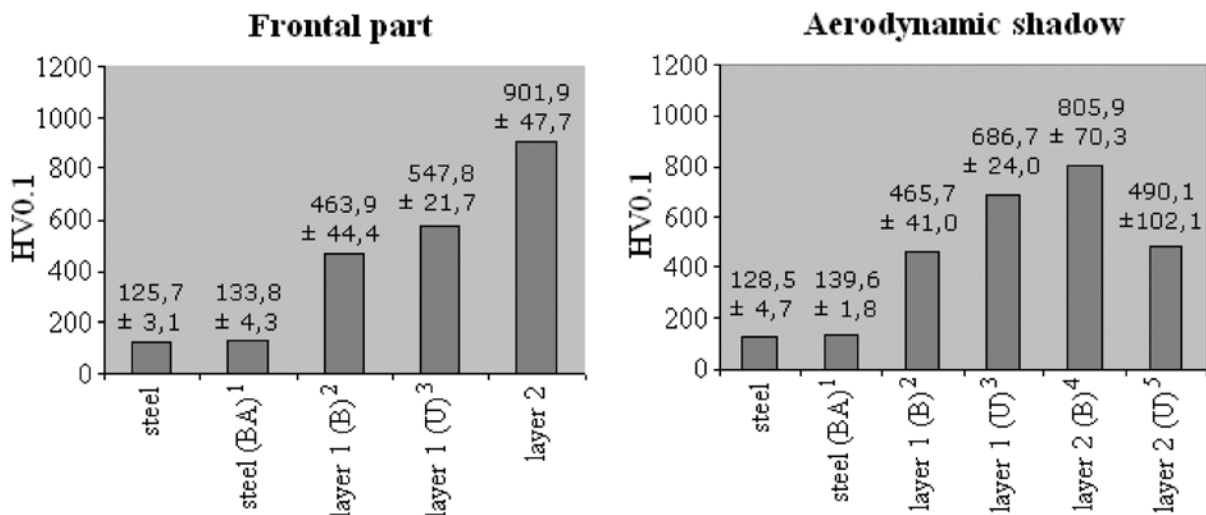
Fig. 4. Phase composition of deposited layers formed on the external surface of steam superheater after prolonged operation: frontal part, aerodynamic shadow

Specimen's hardness was also tested during the analysis; measurements with microhardness were carried out for both steel and individual deposited layers. The study demonstrated that steel hardness was at a medium level, ranging from 125.7 to 128.5 HV0.1. In the boundary zone (up to

ca. 200 μm from steel/deposition boundary) steel showed elevated mean hardness: 133.8 HV0.1 for the first area and 139.6 HV0.1 for the second.

The first layer of the deposition (found previously during microscopic examinations) did not demonstrate high homogeneity in morphological terms. Two parts can be observed in both frontal part and in the aerodynamic shadow: bottom part (B) and upper part (U) of the first layer. In the frontal part, the bottom part of the first layer showed higher porosity compared to the upper part, which was compact and homogeneous. This fact was reflected by the results of hardness tests and standard deviation (Fig. 5). Analogous situation was observed in the case of the first layer in the aerodynamic shadow. Differentiation in hardness in individual microareas and porosity increased with proximity to the steel/deposition boundary.

Due to presence of high-dispersed silicon oxide, the second layer of the deposition in the case of the frontal part was characterized by the highest hardness. Porosity of this layer also contributed to the increase in standard deviation. In the case of the second layer in the aerodynamic shadow, presence of sublayers was observed: lower porous sublayer with hardness of 805.9 HV0.1 and upper sublayer with numerous inclusions. The size of these inclusions (parts substantially higher than in the case of the frontal part) caused that the measurement was carried out in the matrix. Nevertheless, the hardness of inclusions was determined with the example of the greatest grain containing mainly carbon, silicon and oxide; hardness in this case was 1183.8 HV0.05. Mean results of hardness measurements were presented in Figure 5.



1 - steel in the boundary area steel/deposit; 2 - bottom part of first layer; 3 - upper part of first layer; 4 - bottom part of second layer; 5 - upper part of second layer

Fig. 5. Steel hardness in individual layers of the deposition formed on the external surfach of 10CrMo9-10 steel

5. CONCLUSIONS

- ✓ Prolonged operation caused changes in external topography of the surface of a tube elbow in the steam superheater, leading to corrosion and erosion changes.
- ✓ The deposited layer formed on this component showed varied morphology; in the frontal part steel/deposition boundary and boundaries between individual parts of the deposited layer were irregular, with thickness in certain areas exceeding 600 μm . Deposition in the aerodynamic shadow with thickness reaching ca. 410 μm showed regular boundary lines.
- ✓ Analysis of chemical composition revealed presence of sulphur and alkalis in the deposited layer formed on the surface of 10CrMo9-10 steel coming from the combusted mixtures of fuels. Presence of these elements on the surface of the superheater accelerates corrosion and erosion damages.
- ✓ X-ray examinations revealed presence of oxides in the deposited layer, primarily iron oxides and silicon oxides, iron sulphides and complex phases (CaAl_2O_4 , KNaCO_3), which are derivatives of co-combustion of the mixture of coal and biomass in the final period of superheater operation.
- ✓ Hardness tests revealed varied properties of individual deposited layers, which should be associated with altered morphology of layers and their chemical composition.

6. REFERENCES

- [1] Malko J. *Niepewna przyszłość energetyczna*. Energetyka 2013, 4, pp. 325-238.
- [2] Chmielniak T. *Szanse i bariery w rozwoju technologii energetycznych paliw kopalnych*. Polityka Energetyczna 2011, vol. 14, part 2, pp. 23-34.
- [3] Al-Mansour F., Zuwała J. *An evaluation co-firing in Europe*. Biomass & Bioenergy 2010, 34, pp. 620-629.
- [4] Sidur R., Abdelaziz E.A., Demirbas A., Hossain M.S., Mekhilef S. *A review on biomass as a fuel for boilers*. Renewable and Sustainable Energy Reviews 2011, 15, pp. 2262-2289.
- [5] Chmielniak T. *Węglowe technologie energetyczne 2020+*. Polityka Energetyczna 2010, vol. 13, part 2, pp. 77-89.
- [6] Khan A.A., de Jong W., Jansens P.J., Spliethoff H.: *Biomass combustion in fluidized bed boilers: Potential problems and remedies*, Fuel Processing Technology 2009, 90, pp. 21-50.
- [7] Opydo M., Kobylecki R., Dudek A., Bis Z. *Degradacja powierzchni podgrzewacza wody w kotle energetycznym dużej mocy*. Aktualne zagadnienia energetyki 2014, vol. 2, pp. 379-387.
- [8] Teixeira P., Lopes H., Gulyurtlu I, Lapa N., Abelha P. *Evaluation of slagging and fouling tendency during biomass co-firing with coal in fluidized bed*. Biomass & Bioenergy 2012, 39, pp. 192-203.
- [9] Parikh J., Channiwala S.A., Ghosal G.K. *A correlation for calculating HHV from proximate analysis of solid state*. Fuel 2005, 84, pp. 487-494.
- [10] Kalembkiewicz J., Chmielarz U. *Ashes from co-combustion of coal and biomass: New industrial wastes*. Resources, Conservation and Recycling 2012, 69, pp. 109-121.
- [11] Vassilev S.V., Baxter D., Andersen L.K., Vassileva C.G. *An overview of the composition and application of biomass ash. Part I. Phase-mineral and chemical composition and classification*. Fuel 2013, 105, pp. 40-76.